

Magnetohydrodynamic dissipation range spectra for isotropic viscosity and resistivity

P. W. Terry and V. Tangri

*Center for Magnetic Self Organization in Laboratory and Astrophysical Plasmas,
University of Wisconsin-Madison, Madison, Wisconsin 53706, USA*

(Received 22 June 2009; accepted 20 July 2009; published online 11 August 2009)

Dissipation range spectra for incompressible magnetohydrodynamic turbulence are derived for isotropic viscosity μ and resistivity η . The spectra are obtained from heuristic closures of spectral transfer correlations for cases with $Pm = \mu/\eta \leq 1$, where Pm is the magnetic Prandtl number. Familiar inertial range power laws are modified by exponential factors that dominate spectral falloff in the dissipation range. Spectral forms are sensitive to alignment between flow and magnetic field. There are as many as four Kolmogorov wavenumbers that parametrize the transition between inertial and dissipative behavior and enter corresponding spectral forms. They depend on the values of the viscosity and resistivity and on the nature of alignment in inertial and dissipation ranges.

© 2009 American Institute of Physics. [DOI: [10.1063/1.3200901](https://doi.org/10.1063/1.3200901)]

I. INTRODUCTION

Observations of magnetic turbulence in the solar wind,^{1,2} the aurora,³ and laboratory plasmas⁴ have accessed high frequencies, or equivalently, large wavenumbers. The spectra appear to have breaks, with ensuing ranges of steeper power law (increasing spectral index). The range beyond the first break is sometimes labeled a dissipation range (see Ref. 3 for example). The designation “dissipative” should be taken as tentative, indicating a regime of different physics (relative to lower frequencies) that may be due to dissipation, or to some new set of inertial effects. For example, near the Larmor radius scale, inertial-range magnetohydrodynamic (MHD) turbulence transitions to inertial-range kinetic Alfvén wave turbulence with a steeper spectral index, provided fluctuations remain inertial.^{5–7} However, it is well known that in Navier-Stokes turbulence the transition to the dissipation range at the Kolmogorov scale leads to a range of exponential falloff. Exponential falloff can be represented as a sequence of power law spectra with ever increasing spectral index.⁸ Over a wavenumber range limited to something like a decade on a log-log plot, exponential falloff can appear to be a sequence of two power laws connected at a knee.

As a reference for observed spectra in wavenumber ranges where the dissipation becomes dynamically important and falloff becomes exponential, it would be useful to have a spectrum model for MHD with that form of decay. Using model spectra with exponential falloff in such ranges is more physically meaningful for characterizing observed spectral variation than sequences of steeper power laws. Exponentially decaying dissipation range spectra for MHD have received only passing mention,^{9,10} and, as far as we know, have not been derived. We begin here the process by considering dissipation range spectrum for isotropic viscosity and resistivity. This is a starting point only. There are other dissipative effects beyond isotropic viscosity and resistivity, including anisotropic viscosity, fluctuations driven by velocity space anisotropies, and kinetic dissipation from Landau damping and cyclotron resonance. There is growing evidence that

such effects are present in observed scales for the solar wind, aurora, and other plasmas with evidence of kinetic dissipation. Ultimately, therefore, kinetic effects must be incorporated into dissipation range analyses.

However, in developing dissipation range analysis for magnetic turbulence, there are complications intrinsic to magnetofluids that first warrant consideration under the simpler MHD fluid model with isotropic viscosity. These complications include the differences in behavior associated with variations of the magnetic Prandtl number Pm and the effect of alignment between magnetic field and flow.¹¹ These effects already add complexity in inertial scales. For example, unaligned turbulence produces an inertial range spectrum that decays as $k^{-5/3}$,¹² whereas self-similar scale dependent alignment yields $k^{-3/2}$.¹¹ A third power law, $k^{-11/3}$, applies to the magnetic spectrum above the nominal resistively dissipated wavenumber in turbulence with $Pm < 1$.^{13,14} We examine the transition of these power laws to exponentially dissipated spectrum ranges consistent with the relevant physics. The spectra we derive offer a reference for MHD computation, which remains the most widely solved model for magnetic turbulence. Moreover, the exercise yields a fluid dissipation-range benchmark to which the spectral features of kinetic effects can be compared.

Alignment must be considered in dissipation range analysis because it affects the strength of the nonlinearity. This, in turn, affects the amount of energy that can be dissipated in the time scale of nonlinear spectral transfer between spatial scales. Alignment in the inertial range is postulated to be scale dependent in such a way that it leads to a self-similar depletion of the nonlinearity and a reduction in spectral falloff from $k^{-5/3}$ to $k^{-3/2}$.¹¹ The postulated alignment has been observed in simulation¹⁵ and in solar wind data.¹⁶ Simulations also indicate that alignment ceases to be scale dependent in the dissipation range, with the mean angle between fields that holds at the Kolmogorov scale remaining frozen in for smaller scales.¹⁷ These results are empirical and not understood from first principles. Consequently we eval-

ate dissipation range spectra for turbulence that is both aligned and unaligned. These two cases must be calculated even for the aligned turbulence described in Ref. 17 because dissipation occurs for scales both larger and smaller than the Kolmogorov scale, while the nature of alignment changes from scale dependent to scale independent. Alignment and nonalignment have been related to inertial structures that are sheetlike and filamentlike respectively. Formulation of dissipation range spectra allows us to draw inferences regarding the nature and anisotropy of dissipative structures.

The magnetic Prandtl number is the ratio of viscosity to resistivity and is a critical parameter for magnetic dissipation range turbulence. Regimes with $Pm \neq 1$ obviously have unequal dissipation rates and distinct wavenumbers for which the kinetic and magnetic energies transition away from inertial ranges. More subtly, the transition from the inertial ranges for $Pm=1$ is amenable to treatments that are similar to those of Navier–Stokes turbulence, whereas the transition for $Pm \neq 1$ must account for nonlocal wavenumber interactions.^{13,14} These considerations enter the closure of the third order correlations that govern energy transfer.

Even for Navier–Stokes turbulence, with its single form of dissipation and its unique Kolmogorov scale, there are a rather large number of dissipation range theories arising from different approaches to the closure problem.^{18–24} These approaches employ a variety of disparate modeling techniques and approximations, from mean-shear representations for turbulent straining¹⁸ to statistical closure theory,²² to name just two. All yield spectra of the form

$$E(k) = a\epsilon^{2/3}k^{-5/3} \exp[-b(k/k_{dis})^\alpha], \quad (1)$$

where k is the wavenumber, ϵ is the turbulent dissipation rate, k_{dis} is the Kolmogorov wavenumber, and a and b are constants of order unity. The value of α depends on the turbulence model and associated closure approximation and ranges from 1 to 2. For data that do not extend more than a decade in k beyond k_{dis} , all exponents with $1 < \alpha < 2$ provide reasonable fits to measured spectrum shapes.²⁵ This paper does not attempt to address the complex problem of which of seven closure calculations of the Navier–Stokes problem might best apply to magnetic turbulence. Rather, we restrict ourselves to simple, physically transparent closures, checking them against known asymptotic limits, so that we can focus instead on how magnetic properties like alignment and unequal dissipation of turbulent fields carry into the dissipation range.

For $Pm=1$ a simple hydrodynamic closure²¹ can be extended to MHD and allows examination of aligned and unaligned turbulence. The theory is based on a physically appealing closure assumption that amounts to having transferred spectral power at k decrease by the energy lost to dissipation during an eddy turnover time. In hydrodynamics this results in a spectrum with $\alpha=4/3$. An equivalent spectral law was derived by Corrsin¹⁹ and Pao.²⁰ In certain analyses of hydrodynamic data, $\alpha=4/3$ appears to best capture the large Reynolds number limit.²⁵ However, other analyses indicate $\alpha=1$ is preferable.²⁶ The hydrodynamic closure specifies the inertial power law as an asymptote for long wavelengths and recovers the spectrum across the full dynamic

range $0 < k < \infty$. It yields an expression for the Kolmogorov wavenumber as the scale at which exponential behavior dominates falloff. The expression reproduces the results of the standard derivation. The analysis can be applied in a straightforward fashion to unaligned turbulence. For aligned turbulence the analysis can be adapted by supplying the scale dependence of the alignment angle. We calculate the dissipation range spectrum of aligned turbulence using the empirical alignment angle of MHD simulations.^{17,27} Because alignment reduces the strength of the nonlinearity, it also changes the Kolmogorov wavenumber. Hence the closures of aligned and unaligned turbulence lead to separate Kolmogorov wavenumbers.

For $Pm < 1$, the treatment of the dissipation range must account for the dissipative balance and nonlocal transfer that yields the $k^{-11/3}$ spectrum for magnetic energy above the resistive Kolmogorov wavenumber.^{13,14} The hydrodynamic closure²¹ is too simple, but its description of the attenuation of spectrally transferred energy by dissipation can be used with the dissipative balance and nonlocal analysis of Refs. 13 and 14 to impose the proper asymptotic behavior as the wavenumber approaches the resistive Kolmogorov wavenumber from above. The result is again a spectrum over the full dynamic scale range with dissipative and inertial limits. This spectrum carries imprints of the separate Kolmogorov wavenumbers for viscosity and resistivity. Moreover, if there is inertial alignment, there are Kolmogorov wavenumbers for all combinations of alignment and dissipation.

For $Pm > 1$, the heuristic closures used in the other two limits are inadequate. In the hydrodynamic closure the transfer rate stresses that govern the dissimilar spectra for magnetic field and flow are represented by the same dimensional form. To treat this regime, the stresses must be modeled in a way that accounts for differences between $\mathbf{v} \cdot (\mathbf{B} \cdot \nabla) \mathbf{B}$, $\mathbf{B} \cdot (\mathbf{v} \cdot \nabla) \mathbf{B}$, and $\mathbf{B} \cdot (\mathbf{B} \cdot \nabla) \mathbf{v}$, where \mathbf{B} and \mathbf{v} are the turbulent magnetic and flow fields. This requires the analysis of moment equations beyond the energy moments considered here. This more difficult limit is left to future work.

This work is organized as follows. In Sec. II we describe the dissipation range theory, which is based on analysis of spectral energy transfer in the presence of dissipation. In Sec. III we derive MHD dissipation range spectra for $Pm < 1$ and $Pm=1$, and for aligned and unaligned turbulence. Section IV gives conclusions.

II. DISSIPATION RANGE ENERGY TRANSFER

The resistive incompressible MHD equations are

$$\frac{\partial \mathbf{v}}{\partial t} + \mathbf{v} \cdot \nabla \mathbf{v} - \mathbf{B} \cdot \nabla \mathbf{B} = -\nabla \left[p + \frac{B^2}{2} \right] + \mu \nabla^2 \mathbf{v}, \quad (2)$$

$$\frac{\partial \mathbf{B}}{\partial t} + \mathbf{v} \cdot \nabla \mathbf{B} - \mathbf{B} \cdot \nabla \mathbf{v} = \eta \nabla^2 \mathbf{B}, \quad (3)$$

where η is the resistivity, μ is the isotropic viscosity, and the remaining symbols have their usual meanings. A factor $1/\sqrt{4\pi\rho}$ has been absorbed into the variable \mathbf{B} , where ρ is the mass density. The form of the dissipation is idealized, even in the context of fluid theory. Analysis of collisional

processes yields anisotropic viscosity when there is a strong guide field.²⁸ Nonetheless, Eqs. (2) and (3) are a standard model, especially for simulations of magnetic turbulence.

In the inertial range the nonlinearities transfer energy spectrally to higher wavenumber with essentially no loss of energy, i.e., the scales are sufficiently large to make the dissipative terms negligible. In the dissipation range the nonlinearities continue to transfer energy spectrally, but now, viscous and resistive energy dissipation rates exceed the nonlinear rates of energy transfer. The result is that energy available for spectral transfer is attenuated as it progresses to higher wavenumber at rates governed by the viscosity and resistivity. This is expressed by

$$-2\mu E_v(k)k^2 = \frac{dT_v}{dk}, \quad (4)$$

$$-2\eta E_B(k)k^2 = \frac{dT_B}{dk}, \quad (5)$$

where $E_v(k)$ and $E_B(k)$ are the spectral power densities associated with flow and magnetic field fluctuation, defined by $E_v(k)=\int v^2 \exp[i\mathbf{k}\cdot\mathbf{x}]d^3x$ and $E_B(k)=\int B^2 \exp[i\mathbf{k}\cdot\mathbf{x}]d^3x$. The spectral energy transfer rates $T_v(k)$ and $T_B(k)$ are

$$T_v(k) = \int \{\mathbf{v} \cdot (\mathbf{v} \cdot \nabla) \mathbf{v} - \mathbf{v} \cdot (\mathbf{B} \cdot \nabla) \mathbf{B}\} \exp[i\mathbf{k}\cdot\mathbf{x}] d^3x, \quad (6)$$

$$T_B(k) = \int \{\mathbf{B} \cdot (\mathbf{v} \cdot \nabla) \mathbf{B} - \mathbf{B} \cdot (\mathbf{B} \cdot \nabla) \mathbf{v}\} \exp[i\mathbf{k}\cdot\mathbf{x}] d^3x. \quad (7)$$

If the transfer rates can be expressed as functions of $E_v(k)$ and $E_B(k)$, Eqs. (4) and (5) can be solved for the form of the spectral densities. The matter of expressing T_v and T_B in terms of E_v and E_B is the closure problem mentioned in the Introduction.

A. $\text{Pm}=1$

We consider first situations in which the magnetic Prandtl number Pm is unity, i.e., $\mu=\eta$. This regime is frequently assumed in computation. It makes sense to use Elsässer variables, $\mathbf{Z}_+ = \mathbf{v} + \mathbf{B}$ and $\mathbf{Z}_- = \mathbf{v} - \mathbf{B}$. Adopting a compact notation \mathbf{Z}_\pm for the two variables, the two MHD equations are compactly expressed as

$$\frac{\partial \mathbf{Z}_\pm}{\partial t} + \mathbf{Z}_\pm \cdot \nabla \mathbf{Z}_\pm = -\nabla \left[p + \frac{B^2}{2} \right] + \eta \nabla^2 \mathbf{Z}_\pm. \quad (8)$$

The transfer attenuation balances are

$$-2\eta E_\pm k^2 = \frac{dT_\pm}{dk}, \quad (9)$$

where $E_\pm(k)=\int Z_\pm^2 \exp[i\mathbf{k}\cdot\mathbf{x}]d^3x$. The hydrodynamic closure we use²⁹ treats the problem dimensionally, leading us to write

$$T_\pm(k) = Z_\pm^2 Z_+ \Theta_k k. \quad (10)$$

Because Eq. (10) is written in terms of vector magnitudes, whereas the transfer rates involves vector products $\mathbf{Z}_\pm \cdot \nabla \mathbf{Z}_\pm$, there is an alignment factor Θ_k . If this factor is

unity for all k , we will refer to the fields as unaligned. In this situation \mathbf{Z}_+ and \mathbf{Z}_- are perpendicular, an orientation that maximizes the nonlinearity. For $\Theta_k=1$ the inertial range spectrum of Goldreich and Sridhar¹² are recovered. In fact, to recover the Goldreich–Sridhar spectrum, Θ_k need not be unity, but only constant (independent of k). In the so-called aligned case, $\Theta_k < 1$ and decreases with k , yielding a depletion of the nonlinearities and nonlinear transfer rates.¹¹ In the inertial range the scale-dependent reduction is assumed to be self-similar across scales. This means it is proportional to a power of k . If Θ_k is proportional to $k^{-1/4}$ the reduction reproduces the spectrum of Iroshnikov and Kraichnan.^{29,30} However, unlike the assumptions made in Refs. 29 and 30, the fluctuations are anisotropic. In addition to the usual stretching along the mean field, eddies are oblate in the plane perpendicular to the mean field. This produces the partial alignment of \mathbf{Z}_+ and \mathbf{Z}_- responsible for the depletion of the nonlinearity as described by Θ_k .¹¹ Evidence for this alignment has been observed in simulations.^{17,27}

We now consider the closure of Eq. (10). In the procedure of Ref. 21, Z_\pm^2 is replaced by $E_\pm(k)k$, while the remaining factors are expressed as functions of k , using the inertial Obukov balance [$\epsilon=T_\pm(k)$] that yields the inertial range spectrum. This step effectively builds into the analysis the proper inertial limiting behavior for wavenumbers that are much smaller than the Kolmogorov wavenumber. For unaligned turbulence, this means $\Theta_k=1$ and $\mathbf{Z}_\pm = \epsilon^{1/3}/k^{1/3}$, where ϵ is the inertial range dissipation rate. Therefore,

$$T_\pm = E_\pm(k) \epsilon^{1/3} k^{5/3} \quad (\text{unaligned}). \quad (11)$$

This closure does not represent a unique prescription for writing T_\pm in terms of E_\pm . For example, alternate closures can be generated by geometrically splitting Z_\pm^2 into a part that is converted to E_\pm and a part that is written as a function of k using the inertial range spectrum

$$T_\pm(k) = Z_\pm^2 Z_+ k = [Z_\pm^2]^\delta [Z_+]^{1-\delta} Z_+ k = E_\pm^\delta(k) \epsilon^{1-2\delta/3} k^{5\delta/3}. \quad (12)$$

Only for $\delta=1$ is an exponential spectrum generated. Moreover, this is the only choice that asymptotes to the correct inertial range spectrum for scales that are larger than the Kolmogorov scale. These important physical features therefore dictate the choice $\delta=1$.

For aligned turbulence the closure is handled similarly, again with $\delta=1$. Here, however, Θ_k is different from unity and must be specified as a function of k . The inertial-range Iroshnikov–Kraichnan spectrum, $E=\epsilon^{1/2} V_A^{1/2}/k^{3/2}$, implies that $Z_+ = \epsilon^{1/4} V_A^{1/4}/k^{1/4}$, where $V_A=B_0/\sqrt{4\pi\rho}$. Both of these relations are recovered from the Obukov inertial balance if

$$\Theta_k = \epsilon^{1/4}/V_A^{3/4} k^{1/4}. \quad (13)$$

This scale-dependent angle is formally an inertial range construct. It is not derived from first principles, but postulated as the form that yields the Iroshnikov–Kraichnan power law observed in simulations. Thus it is an empirical relation. Without a theoretical base, it is not obvious how to theoretically predict the behavior of the angle Θ_k in the dissipation range. The simplest assumption would be that the nonlinear

physics that reduces Θ_k with increasing k as described by Eq. (13) continues unchanged into the dissipation range. This is the essence of the hydrodynamic dissipation range as described by Eq. (1), because the self-similar power-law factor continues in force even as its decay is overwhelmed by the exponential factor. However, it is also possible that the additional complexities of MHD break this symmetry. There is evidence for the latter possibility in the simulations of Ref. 17, which access the dissipation range. Figure 2 of Ref. 17 shows that the reduction in Θ_k saturates at the wavenumber $k=k_{\eta_{al}}$ of the transition to the dissipation range, asymptoting to the constant value

$$\Theta_k = \epsilon^{1/4}/V_A^{3/4} k_{\eta_{al}}^{1/4} \quad \text{for } k \geq k_{\eta_{al}}, \quad (14)$$

Here, the transition wavenumber $k_{\eta_{al}}$ has a subscript to indicate the type of dissipation that induces the transition and whether or not the inertial fluctuations are aligned. This wavenumber will naturally emerge from the spectrum calculation in the next section as the wavenumber at which dissipative forces become equal to inertial forces. This makes $k_{\eta_{al}}$ a Kolmogorov wavenumber. We will not attempt to address whether the dissipation range is fully resolved in Ref. 17. Rather, we will take the results at face value and calculate the spectrum consistent with the variation shown in Fig. 2 of Ref. 17. As shown in the next section it is trivial to modify the spectrum for the hypothetical case in which Eq. (13) continues to hold in the dissipation range.

To determine $T_{\pm}(k)$ consistent with Eq. (13) for $k < k_{\eta_{al}}$ and Eq. (14) for $k \geq k_{\eta_{al}}$, we use Eq. (10) for $T_{\pm}(k)$. The field Z_{\pm} is determined from the Obukov balance $\epsilon = Z_{\pm}^3 \Theta_k k$. This yields

$$T_{\pm}(k) = \frac{E_{\pm}(k) \epsilon^{1/2} k^{3/2}}{V_A^{1/2}} \quad \text{for } k < k_{\eta_{al}}, \quad (15)$$

$$T_{\pm}(k) = \frac{E_{\pm}(k) \epsilon^{1/2} k^{5/3}}{V_A^{1/2} k_{\eta_{al}}^{1/6}} \quad \text{for } k \geq k_{\eta_{al}}, \quad (16)$$

for aligned turbulence.

The unaligned and aligned cases of MHD turbulence included above represent two paradigms for inertial range spectra that dominated thinking about MHD turbulence over the years. We consider the type of fluctuation structure they represent in the inertial and dissipation ranges. Because $\Theta_k = 1$ implies $\mathbf{Z}_+ \perp \mathbf{Z}_-$, unaligned turbulence has comparable scales k_{\perp}^{-1} in the plane perpendicular to the mean field. The elongation of eddies along the field ($k_{\parallel} \ll k_{\perp}$) yields structures that are filamentlike. With equal dissipation of v and B , and the assumption that $\Theta_k = 1$ continues to hold in the dissipation range, the structures remain filamentlike. For aligned turbulence, Eq. (13) implies that the angle between \mathbf{Z}_+ and \mathbf{Z}_- becomes smaller with increasing k , introducing a small scale $k_{\perp}^{-1} \Theta_k$ in one direction in the plane perpendicular to the mean field and k_{\perp}^{-1} in the other direction. The elongation along the field then yields sheetlike structures. Figure 2 of Ref. 17 indicates that the transverse aspect ratio of the sheets becomes fixed in the dissipation range. Additional dissipative effects in plasmas beyond simple resistivity and vis-

cosity, including Landau damping, gyroresonant damping, and anisotropic viscosity, may modify fluctuation structure.

B. $Pm < 1$

In Sec. II A we found closed expressions for $T_{\pm}(k)$, valid for $Pm=1$. These expressions, both for unaligned and aligned turbulence, are also applicable to $Pm < 1$ for inertial scales where nonlinear processes dominate. The transfer rates for unaligned turbulence, $T_{\pm}(k) = E_{\pm}(k) \epsilon^{1/3} k^{5/3}$, may also be represented in the original v and B variables as

$$T_v(k) = E_v(k) \epsilon^{1/3} k^{5/3}, \quad (17)$$

$$T_B(k) = E_B(k) \epsilon^{1/3} k^{5/3} \quad (k < k_{\eta_{un}}), \quad (18)$$

where $k_{\eta_{un}}$ is the wavenumber at which the resistive dissipation rate becomes equal to the nonlinear time scale, when turbulence is not aligned. It will be derived in the next section from the spectrum forms. Equations (17) and (18) can be obtained by transformation from T_{\pm} assuming balanced turbulence ($E_+ = E_-$), or from the hydrodynamic closure of Eqs. (6) and (7), with $B^2 \rightarrow E_B(k)k$, $v^2 \rightarrow E_v(k)k$, and taking $B^2 = v^2$ in the second nonlinearity of Eq. (6).

In the dissipation range, the magnetic field is dissipated at a rate that exceeds the transfer rate, while the flow remains inertial. This results in $B \ll v$. The dynamics are no longer Alfvénic but resemble Navier–Stokes turbulence for the flow. Magnetic field dynamics are parasitic on the flow, but not through Alfvénic interactions. The closure must reflect the different physics of this regime. With $B \ll v$ there is no advantage conferred by Elsässer variables, hence we use the standard MHD fields. For $B \ll v$, the dimensional forms of T_v and T_B from Eqs. (6) and (7) become $T_v(k) = v^3 k$ and $T_B = B^2 v k$. Because $T_v(k)$ is purely kinetic and dominates transfer, kinetic energy continues in its inertial range. This makes Eq. (17) valid not just for $k < k_{\eta_{un}}$ but for all k . Under the hydrodynamic prescription the factor B^2 in the magnetic transfer rate T_B is replaced by $E_B(k)k$. This is essentially a local representation of turbulent interactions between coupled Fourier modes because T_B is treated as a function of a single wavenumber k . For isotropic and homogeneous hydrodynamic turbulence, this is a reasonable approximation. Magnetic turbulence, on the other hand, has significant non-local interactions associated with Alfvénic dynamics. Such nonlocal interactions involving B lead to a known regime of 11/3 power law falloff for magnetic energy in the range between resistive and viscous Kolmogorov wavenumbers.^{13,14}

To see how this regime arises consider the magnetic nonlinearity of Eq. (3), $(v \cdot \nabla) \mathbf{B} - (\mathbf{B} \cdot \nabla) v \rightarrow i \mathbf{v}_{k'} \cdot (\mathbf{k} - \mathbf{k}') \mathbf{B}_{k-k'} - i \mathbf{B}_{k'} \cdot (\mathbf{k} - \mathbf{k}') \mathbf{v}_{k-k'}$. The field $\mathbf{B}_{k'}$ can be a large-scale field in the inertial range $k < k_{\eta_{un}}$, with $\mathbf{v}_{k-k'}$ a flow field in the range $k_{\eta_{un}} < k < k_{\mu_{un}}$, where $k_{\mu_{un}}$ is the viscous Kolmogorov scale. (Like $k_{\eta_{un}}$, the definition of $k_{\mu_{un}}$ will emerge naturally from the spectrum forms derived in the next section.) With this nonlocal interaction $\mathbf{B}_{k'} \cdot (\mathbf{k} - \mathbf{k}') \mathbf{v}_{k-k'}$ dominates the contribution $\mathbf{v}_{k'} \cdot (\mathbf{k} - \mathbf{k}') \mathbf{B}_{k-k'}$ because $\mathbf{B}_{k-k'} \ll \mathbf{v}_{k-k'}$, while $\mathbf{B}_{k'} \sim \mathbf{v}_{k'}$. For the same reason this interaction dominates contributions from local triads in the range $k_{\eta_{un}} < k < k_{\mu_{un}}$. Balancing this nonlinearity with dissipation,

$$\mathbf{B}_{k'} \cdot (\mathbf{k} - \mathbf{k}') \mathbf{v}_{k-k'} \sim (\mathbf{B}_{k'} \cdot \mathbf{k}) \mathbf{v}_k \sim \eta k^2 \mathbf{B}_k. \quad (19)$$

This leads directly to the spectrum

$$E_B(k) = \frac{B_k^2}{k} = \frac{B_{k'}^2}{\eta^2 k^2} \left(\frac{v_k^2}{k} \right) = \frac{B_{k'}^2}{\eta^2 k^2} E_v(k) = \frac{\epsilon^{2/3} B_{k'}^2}{\eta^2 k^{11/3}}, \quad (20)$$

where $E_v(k)$ is the inertial range spectrum for the flow. We used $\epsilon^{2/3} k^{-5/3}$ for the flow spectrum because, with $B \ll v$, the flow is governed by shear straining $[(\mathbf{v} \cdot \nabla) \mathbf{v}]$ and is therefore essentially the flow of Navier-Stokes turbulence. The spectrum of Eq. (20) supplants the inertial range spectrum for $k_{\eta_{un}} < k < k_{\mu_{un}}$. These expressions will be seen to be equivalent to the standard expressions derived from the usual balance of eddy turnover and dissipation rates.

The above analysis can be extended beyond $k_{\eta_{un}} < k < k_{\mu_{un}}$ to the viscous dissipation range $k > k_{\mu_{un}}$. Transfer of flow energy is governed by $T_v = v^3 k$ with $v^3 \rightarrow [E_v(k)k] \times [\epsilon^{1/3}/k^{1/3}]$. In the hydrodynamic closure this gives $T_v(k) = E_v(k) \epsilon^{1/3} k^{5/3}$, reproducing Eq. (17). This expression will be used in Eq. (4) in the next section to obtain the spectrum for $E_v(k)$. To obtain E_B the hydrodynamic procedure must be modified to incorporate the nonlocal interaction leading to Eq. (20). The spectrum is no longer determined from Eq. (5), but is obtained from the same balance leading to Eq. (20), which we write as

$$T_B(k) = \eta k^2 B_k^2. \quad (21)$$

Here $T_B(k)$ is evaluated using the nonlocal triad leading to Eq. (20), i.e.,

$$T_B(k) = B_k B_{k'} k v_k = B_k B_{k'} k [E_v(k)k]^{1/2}. \quad (22)$$

Because $k > k_{\mu_{un}}$ is a dissipation range for both kinetic and magnetic energies, $E_v(k)$ is not the inertial range spectrum used in Eq. (20), but is the dissipation range spectrum obtained from the solution of Eq. (4) with Eq. (17).

The kinetic energy transfer rate [Eq. (17)] is the same as the transfer rates for unaligned turbulence derived in the previous subsection. However, alignment or lack thereof is not what fixes its form. Rather, it follows from the Obukov balance when the energy containing field is \mathbf{v} , as it must be for $v \gg B$. Nevertheless, if turbulence is unaligned in the inertial range, $k < k_{\eta_{un}}$, the identical form of $T_v(k)$ for $k > k_{\eta_{un}}$ will give identical spectra in both regions. If, however, the turbulence is aligned in the inertial range, the flow spectrum will have different power-law factors below and above the resistive Kolmogorov wavenumber. This wavenumber, in turn, will be indexed to aligned inertial behavior.

Turbulence with $Pm=1$ is characterized by either sheet-like or filamentlike structures, depending on alignment. Both types of structure are oriented along the guide field. For $Pm < 1$ these two possibilities also arise, but only for the inertial scales. Beyond the resistive Kolmogorov scale, fluid streaming $[(\mathbf{v} \cdot \nabla) \mathbf{v}]$ dominates the nonlinear dynamics responsible for carrying energy to smaller scale, producing the filamentary structures of Navier-Stokes turbulence. The weak magnetic field at these scales is slaved to the flow through Eq. (19) and does not act back on the flow. Therefore these filaments, while they carry a field, become dy-

namically independent from it and do not align with the guide field. These filaments are the characteristic structures of both \mathbf{v} and \mathbf{B} beyond the resistive Kolmogorov scale.

C. $Pm > 1$

For $Pm > 1$ there is a range for which v decays exponentially while B remains subject to inertial transfer, resulting in $v \ll B$. The dimensional treatment of Eqs. (6) and (7) yields $T_v = T_B = B^2 v k$. The equality of T_v and T_B overconstrains the attenuation balances [Eqs. (4) and (5)] when $\mu \neq \eta$. Moreover, the differences between T_v and T_B in Eqs. (6) and (7) are not amenable to the same simple nonlocal dimensional analysis that was used for $Pm < 1$. Rather the range between the viscous and resistive Kolmogorov wavenumbers can be treated as a problem in passive advection.³¹ The analysis has been done, leading to a magnetic spectrum that decays as k^{-1} .¹⁰ However for the range above the resistive Kolmogorov wavenumber it is not clear how to incorporate the exponential correction using any of the heuristic approaches of this paper. The more complex closure analysis required will be treated in the future.

III. DISSIPATION RANGE SPECTRA

The closed energy transfer expressions obtained in the previous section can now be used to derive spectra. We consider separately the regimes for $Pm=1$ and $Pm < 1$. Within those parametrizations we also consider both unaligned and scale-dependent aligned turbulence. Growing evidence favors the latter, but we also do the former because it is a simpler extension from Navier-Stokes turbulence and informs the considerations necessary for the aligned case.

A. $Pm=1$

1. Unaligned turbulence

For unaligned turbulence the spectra are obtained from Eqs. (9) and (11), which yield the differential equation,

$$-2\eta E_{\pm}(k)k^2 = \frac{d}{dk} [E_{\pm}(k) \epsilon^{1/3} k^{5/3}]. \quad (23)$$

The solution of this equation is $E_{\pm}(k) = a \epsilon^{2/3} k^{-5/3} \times \exp[-(3/2) \eta k^{4/3} / \epsilon^{1/3}]$, where a is a constant of integration. If we put the argument of the exponent in the form $[-(3/2) \times (k/k_{\eta_{un}})^{4/3}]$, we obtain

$$E_{\pm}(k) = a \epsilon^{2/3} k^{-5/3} \exp \left[-\frac{3}{2} \left(\frac{k}{k_{\eta_{un}}} \right)^{4/3} \right] \quad (\text{unaligned}), \quad (24)$$

with

$$k_{\eta_{un}} = \frac{\epsilon^{1/4}}{\eta^{3/4}}. \quad (25)$$

We recognize this parameter combination as the Kolmogorov wavenumber of Navier-Stokes turbulence, with η in the place of μ ($\eta=\mu$ for $Pm=1$). Solution of the wavenumber attenuation balances of Eqs. (4) and (5) generally has the property that the Kolmogorov wavenumber is recovered

from the dimensional scaling of the exponential factor. This is true for both unaligned and aligned cases.

2. Aligned turbulence

For aligned turbulence Eqs. (9), (15), and (16) yield

$$-2\eta E_{\pm}(k)k^2 = \frac{d}{dk} \left[\frac{E_{\pm}(k)\epsilon^{1/2}k^{3/2}}{V_A^{1/2}} \right] \quad (k < k_{\eta_{al}}), \quad (26)$$

$$-2\eta E_{\pm}(k)k^2 = \frac{d}{dk} \left[\frac{E_{\pm}(k)\epsilon^{1/2}k^{5/3}}{V_A^{1/2}k_{\eta_{al}}^{1/6}} \right] \quad (k \geq k_{\eta_{al}}). \quad (27)$$

The solution of Eq. (26) is $E_{\pm}(k) = a_{<} \epsilon^{1/2} V_A^{1/2} k^{-3/2} \times \exp[-(4/3)\eta k^{3/2} V_A^{1/2} / \epsilon^{1/2}]$, where $a_{<}$ is a constant of integration. We again introduce a wavenumber $k_{\eta_{al}}$ as the parameter combination that puts the argument of the exponent of E_{\pm} in the form $[-(4/3)(k/k_{\eta_{al}})^{3/2}]$. This yields

$$k_{\eta_{al}} = \frac{\epsilon^{1/3}}{V_A^{1/3} \eta^{2/3}}. \quad (28)$$

This is identical to the Kolmogorov wavenumber for aligned turbulence derived in the usual way. (The usual derivation sets the nonlinearity equal to the dissipative term, including depletion due to alignment. The inertial range spectrum power law is used to specify the wavenumber dependence of the amplitude. The expression is then solved for wavenumber.) In terms of $k_{\eta_{al}}$ the spectrum is given by

$$E_{\pm}(k) = a_{<} \epsilon^{1/2} V_A^{1/2} k^{-3/2} \exp \left[-\frac{4}{3} \left(\frac{k}{k_{\eta_{al}}} \right)^{3/2} \right] \quad (k < k_{\eta_{al}}). \quad (29)$$

The solution of Eq. (27) is $E_{\pm}(k) = a_{>} k^{-5/3} \times \exp[-(3/2)\eta k^{4/3} V_A^{1/2} k_{\eta_{al}}^{1/6} / \epsilon^{1/2}]$, where $a_{>}$ is a second constant of integration. The expression for $k_{\eta_{al}}$ defined above also puts the argument of the exponent in the consistent form $[-3/2(k/k_{\eta_{al}})^{4/3}]$. The constant $a_{>}$ is chosen to make the two spectra derived for $k < k_{\eta_{al}}$ and $k \geq k_{\eta_{al}}$ continuous at $k = k_{\eta_{al}}$, yielding

$$E_{\pm}(k) = a_{<} \epsilon^{1/2} V_A^{1/2} k^{-5/3} k_{\eta_{al}}^{1/6} e^{1/6} \exp \left[-\frac{3}{2} \left(\frac{k}{k_{\eta_{al}}} \right)^{4/3} \right] \quad (k \geq k_{\eta_{al}}). \quad (30)$$

Spectrum for turbulence with $\text{Pm}=1$ in the unaligned [Eq. (24)] and aligned [Eqs. (29) and (30)] cases is plotted in Fig. 1.

Note that the dissipation range spectrum for aligned turbulence ($k \geq k_{\eta_{al}}$) has the same form as the spectrum for unaligned turbulence. This means that Eq. (30) is the spectrum form whenever the alignment angle does not vary with k , whether it is given by $\pi/2$ (unaligned turbulence) or some smaller value giving a depletion of the nonlinearity. This form therefore accommodates filamentlike or sheetlike structures, but the structures do not change their transverse aspect ratio with scale. The inertial range form for aligned turbulence ($k < k_{\eta_{al}}$) is the form resulting whenever the alignment angle decreases with k as the $1/4$ power. Consequently in the

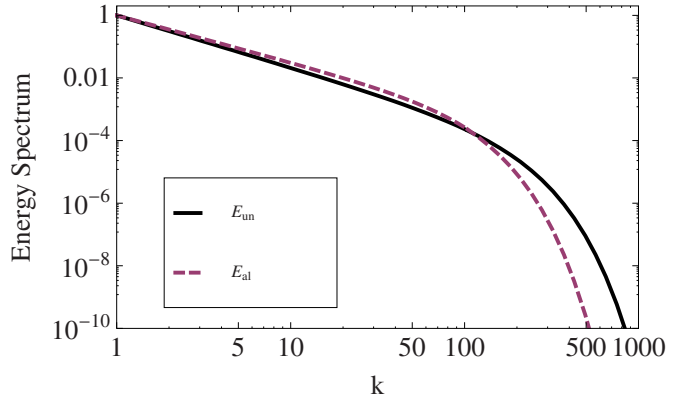


FIG. 1. (Color online) Spectra for aligned MHD turbulence (labeled E_{al}) and unaligned MHD turbulence (labeled E_{un}) for a magnetic Prandtl number of unity. The spectra extend from the inertial range to the dissipation range with $k_{un}=177.8$ and $k_{al}=100$ (in arbitrary units). The aligned turbulence has an alignment angle that decreases with k for $k < k_{al}$ and becomes constant thereafter.

hypothetical case in which $\Theta_k \propto k^{-1/4}$ extends through the whole spectrum, Eq. (29) is the spectrum for aligned turbulence for all wavenumbers.

Both of these spectra can be obtained heuristically by computing the amount of dissipation in an eddy turnover time. To show this, recall that the energy dissipation rate ϵ is the scale-invariant energy transfer rate throughout the inertial range ($\epsilon = T = kv^3 = kB^3$). We estimate how much of this transferred energy is lost to dissipation in an eddy turnover time by calculating the time evolution of resistive decay at wavenumber k in decaying turbulence. Under pure resistive decay

$$B^2 = B_0^2 \exp[-2\eta k^2 t]. \quad (31)$$

For unaligned turbulence the eddy turnover time is $\tau = (vk)^{-1} = \epsilon^{-1/3} k^{-2/3}$. In this time B_0^3 decays to $B_0^3 \times \exp[-3\eta k^{4/3} \epsilon^{-1/3}]$, and ϵ , as a decreasing energy throughput rate, becomes $\epsilon = kB^3 = kB_0^3 \exp[-3\eta k^{4/3} \epsilon^{-1/3}] = \epsilon_0 \times \exp[-3\eta k^{4/3} \epsilon^{-1/3}]$. In an inertial range with an attenuating value of ϵ as just calculated this gives a spectrum $E(k) = \epsilon^{2/3} k^{-5/3} = \epsilon_0^{2/3} k^{-5/3} \exp[-2\eta k^{4/3} \epsilon^{-1/3}] = \epsilon_0^{2/3} k^{-5/3} \times \exp[-2(k/k_{\eta_{un}})^{4/3}]$. This spectrum is not identical to that of Eq. (24), but it has the same wavenumber dependence $(k/k_{\eta_{un}})^{4/3}$ in the argument of the exponential. Hence that dependence is a representation of transferable energy loss in an eddy turnover time. For turbulence with scale dependent alignment ($k < k_{\eta_{al}}$) the eddy turnover time is $\tau = (vk\Theta_k)^{-1} = (\epsilon^{1/4} V_A^{1/4} / k^{1/4})^{-1} k^{-1} (\epsilon^{1/4} / V_A^{3/4} k^{1/4})^{-1} = V_A^{1/2} / \epsilon^{1/2} k^{1/2}$. When this is substituted into Eq. (31), $B^2 = B_0^2 \times \exp[-2\eta V_A^{1/2} k^{3/2} \epsilon^{1/2}] = B_0^2 \exp[-2(k/k_{\eta_{al}})^{3/2}]$, and $\epsilon = B^3 k \Theta_k = B_0^3 k \Theta_k \exp[-3(k/k_{\eta_{al}})^{3/2}] = \epsilon_0 \exp[-3(k/k_{\eta_{al}})^{3/2}]$. When this is used in the aligned inertial spectrum $E(k) = \epsilon^{1/2} V_A^{1/2} k^{-3/2}$, the result is $E(k) = \epsilon_0^{1/2} V_A^{1/2} k^{-3/2} \exp[-(3/2) \times (k/k_{\eta_{al}})^{3/2}]$. Again, the wavenumber dependence of the argument of the exponential in Eq. (29) is recovered.

While this heuristic derivation obviously replicates the mathematical content of the earlier derivation, it is useful in clarifying the reason for the different powers of k in the exponential functions for the cases with and without scale-dependent alignment. Because the depletion of the nonlinear-

ity increases with scale, scale-dependent aligned turbulence decays more gradually in the inertial range than unaligned turbulence ($k^{-3/2}$ instead of $k^{-5/3}$). However the depleted nonlinearity makes the eddy turnover time longer for turbulence with scale-dependent alignment ($\tau \propto k^{-1/2}$ instead of $\tau \propto k^{-2/3}$). Consequently there is more dissipation in an eddy turnover time, and a steeper exponential falloff.

B. $Pm < 1$

For this regime the spectra beyond the resistive Kolmogorov wavenumber will look like those of unaligned turbulence. As discussed in the previous section this is because the Lorentz force becomes negligible, leading to a Kolmogorov spectral index for the flow (unaligned turbulence also follows a Kolmogorov spectral index because of critical balance¹²). The case for unaligned turbulence is therefore simpler because spectrum forms for unaligned turbulence apply on either side of the dissipative wavenumber.

1. Unaligned turbulence

The kinetic energy transfer rate of unaligned turbulence is given by Eq. (17) for all wavenumbers. Substituting into Eq. (4) and solving the differential equation gives

$$E_v(k) = a_{<} \epsilon^{2/3} k^{-5/3} \exp\left[-\frac{3}{2}\left(\frac{k}{k_{\mu_{un}}}\right)^{4/3}\right], \quad (32)$$

where $k_{\mu_{un}}$ is the combination of parameters given by

$$k_{\mu_{un}} = \frac{\epsilon^{1/4}}{\mu^{3/4}}. \quad (33)$$

Likewise, substitution of the magnetic energy transfer rate of Eq. (18) into Eq. (5) yields

$$E_B(k) = a_{<} \epsilon^{2/3} k^{-5/3} \exp\left[-\frac{3}{2}\left(\frac{k}{k_{\eta_{un}}}\right)^{4/3}\right] \quad (k < k_{\eta_{un}}), \quad (34)$$

where $k_{\eta_{un}}$ is given by Eq. (25). Equation (32) is valid for all k , whereas Eq. (34) holds only for $k < k_{\eta_{un}}$. To calculate the magnetic spectrum for $k > k_{\eta_{un}}$ we solve Eq. (21), using the nonlocal expression for the transfer rate [Eq. (22)] and the kinetic energy spectrum, Eq. (32). The result is $E_B(k) = a_{<} \epsilon^{2/3} k^{-5/3} (B_{k'}^2 / \eta^2 k^2) \times \exp[-(3/2)(k/k_{\mu_{un}})^{4/3}]$. The factor $B_{k'}^2$ is the magnetic energy from some inertial scale k' . This factor is part of the balance $(\mathbf{B}_{k'} \cdot \mathbf{k}) \mathbf{v}_k \sim \eta k^2 \mathbf{B}_k$ that mediates the 11/3 power law falloff of B_k^2 above the resistive dissipation scale. The 11/3 power law ensures that the balance holds throughout the range $k > k_{\eta_{un}}$. The scale k' of $B_{k'}$ sets the amplitude of the spectrum for a given value of η . The only constraint on the amplitude is continuity of E_B across $k = k_{\eta_{un}}$. Choosing $B_{k'}^2$ accordingly, the spectrum can be written

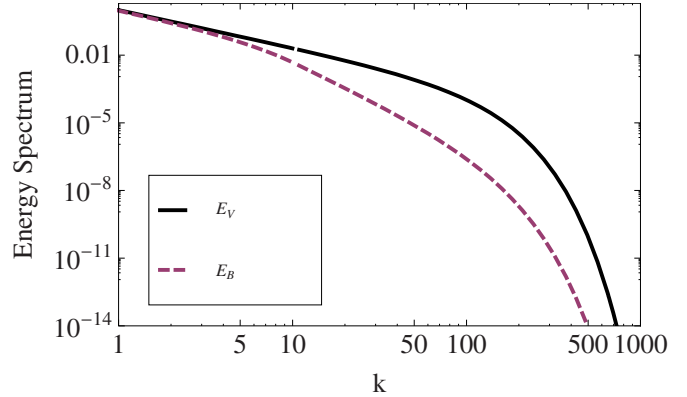


FIG. 2. (Color online) Spectra of magnetic and kinetic energies for unaligned turbulence with $Pm=0.0464$. The resistive and viscous Kolmogorov wavenumbers are $k_{\eta_{un}}=10$ and $k_{\mu_{un}}=100$ (in arbitrary units).

$$E_B(k) = a_{<} \epsilon^{2/3} k^{-11/3} k_{\eta_{un}}^2 \exp\left[-\frac{3}{2}(1-Pm)\right] \times \exp\left[-\frac{3}{2}\left(\frac{k}{k_{\mu_{un}}}\right)^{4/3}\right] \quad (k > k_{\eta_{un}}). \quad (35)$$

Exponential falloff in the magnetic spectrum is governed by resistivity for $k < k_{\eta_{un}}$, whereas for $k > k_{\eta_{un}}$, nonlocal interactions produce an exponential falloff governed by viscosity, with resistivity entering through the factor $k_{\eta_{un}}^2$. The spectra of E_v and E_B for unaligned turbulence are shown in Fig. 2 for a case in which $k_{\mu_{un}}=100$, $k_{\eta_{un}}=10$, and $Pm=(0.1)^{4/3}=4.64 \times 10^{-2}$. Even with only one decade between the resistive and viscous Kolmogorov scales, the magnetic energy becomes significantly smaller in the dissipative scales.

2. Aligned turbulence

Scale-dependent alignment is a property of inertial interactions, even though its observation in simulations has generally been for $Pm=1$. When $Pm < 1$, the magnetic field is dissipated more strongly than the flow, resulting in $B < v$, even in the inertial range. However, the difference is very small in the inertial range. Therefore, alignment should occur much as it does in the $Pm=1$ case. For $Pm=1$, the aligned spectra are given by Eq. (29) in the inertial scales $k < k_{\eta_{al}}$. If we assume balanced turbulence for simplicity [$E_+(k) = E_-(k)$], the spectra for $E_v(k)$ and $E_B(k)$ are the same as those of $E_{\pm}(k)$ given in Eq. (29),

$$E_v(k) = E_B(k) = a_{<} \epsilon^{1/2} V_A^{1/2} k^{-3/2} \exp\left[-\frac{4}{3}\left(\frac{k}{k_{\eta_{al}}}\right)^{3/2}\right] \quad (k < k_{\eta_{al}}, Pm=1). \quad (36)$$

For $Pm < 1$, these spectra have the appropriate form, but E_v and E_B are subject to the different dissipation rates $k^2 \mu$ and $k^2 \eta$. This requires different dissipative wavenumbers for E_v and E_B . These should have the scaling of dissipative wavenumbers for aligned turbulence, giving

$$E_v(k) = a_{<} \epsilon^{1/2} V_A^{1/2} k^{-3/2} \exp\left[-\frac{4}{3}\left(\frac{k}{k_{\mu_{al}}}\right)^{3/2}\right] \quad (k < k_{\eta_{al}}), \quad (37)$$

$$E_B(k) = a_{<} \epsilon^{1/2} V_A^{1/2} k^{-3/2} \exp\left[-\frac{4}{3}\left(\frac{k}{k_{\eta_{al}}}\right)^{3/2}\right] \quad (k < k_{\eta_{al}}). \quad (38)$$

Here $k_{\eta_{al}}$ is given by Eq. (28) and

$$k_{\mu_{al}} = \frac{\epsilon^{1/3}}{V_A^{1/3} \mu^{2/3}}. \quad (39)$$

With $k_{\mu_{al}} > k_{\eta_{al}}$ the exponential correction for E_v is much closer to unity than the already near-unity exponential correction for E_B .

We now consider the range $k > k_{\eta_{al}}$. The flow is governed solely by the nonlinearity $[(\mathbf{v} \cdot \nabla) \mathbf{v}]$. When the corresponding kinetic energy transfer rate [Eq. (17)] is substituted into Eq. (4), we obtain the differential equation $d/dk[E_v k^{1/3} k^{1/3}] = -2\mu E_v(k) k^2$. The solution gives $E_v(k) = a_{>} \epsilon^{2/3} k^{-5/3} \exp[-(3/2)(k/k_{\mu_{un}})^{4/3}]$, where $a_{>}$ is an integration constant and $k_{\mu_{un}}$ is the parameter combination in the argument of the exponential given by Eq. (33). We choose $a_{>}$ to make the spectrum continuous across $k=k_{\eta_{al}}$, yielding

$$E_v(k) = a_{<} \epsilon^{1/2} V_A^{1/2} k_{\eta_{al}}^{1/6} k^{-5/3} \exp\left[-\frac{4}{3}\text{Pm} + \frac{3}{2}\left(\frac{k_{\eta_{al}}}{k_{\mu_{un}}}\right)^{4/3}\right] \\ \times \exp\left[-\frac{3}{2}\left(\frac{k}{k_{\mu_{un}}}\right)^{4/3}\right] \quad (k \geq k_{\eta_{al}}). \quad (40)$$

The wavenumber ratio $k_{\eta_{al}}/k_{\mu_{un}}$ is a dimensionless combination of parameters given by

$$\frac{k_{\eta_{al}}}{k_{\mu_{un}}} = \frac{\mu^{3/4} \eta^{1/12}}{\epsilon^{2/3} V_A^{1/3}} = \text{Pm}^{3/4} \Theta_{k_{\eta_{al}}}^{1/2}, \quad (41)$$

where $\Theta_{k_{\eta_{al}}}$ is the alignment angle Θ_k [Eq. (13)] evaluated at the wavenumber $k_{\eta_{al}}$ that terminates the inertial range. This ratio is small since both Pm and Θ_k are less than unity.

The spectrum for magnetic energy is obtained from Eqs. (21) and (22). We obtain both the known $11/3$ power law spectrum for the range $k_{\eta_{al}} < k < k_{\mu_{un}}$ and the exponential correction that makes the spectrum valid for $k > k_{\mu_{un}}$ by using Eq. (40) for $E_v(k)$ in Eq. (22). The result is

$$E_B(k) = a_{<} \epsilon^{1/2} V_A^{1/2} k_{\eta_{al}}^{1/6} \left(\frac{B_{k'}^2}{\eta^2 k^{11/3}} \right) \exp\left[-\frac{4}{3}\text{Pm} + \frac{3}{2}\left(\frac{k_{\eta_{al}}}{k_{\mu_{un}}}\right)^{4/3}\right] \\ \times \exp\left[-\frac{3}{2}\left(\frac{k}{k_{\mu_{un}}}\right)^{4/3}\right] \quad (k \geq k_{\eta_{al}}). \quad (42)$$

As in the unaligned case, the inertial scale k' that appears in $(\mathbf{B}_{k'} \cdot \mathbf{k}) \mathbf{v}_k \sim \eta k^2 \mathbf{B}_k$ maintains continuity of the spectrum, allowing the spectrum to be rewritten as

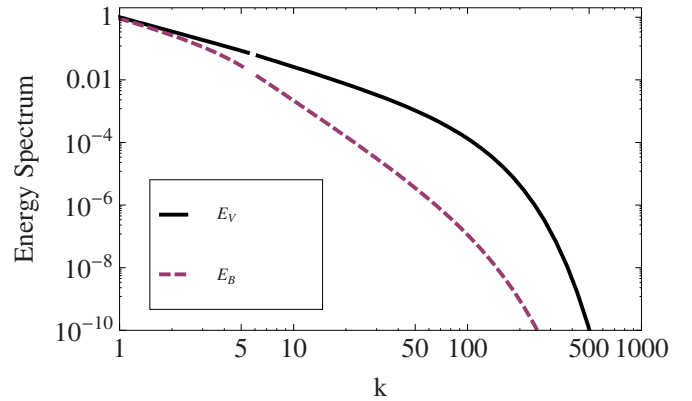


FIG. 3. (Color online) Spectra of magnetic and kinetic energies for aligned turbulence with $\text{Pm}=0.0464$. These spectra depend on resistive and viscous Kolmogorov wavenumbers for both aligned and unaligned turbulence. These wavenumbers are $k_{\eta_{un}}=10$, $k_{\mu_{un}}=100$, $k_{\eta_{al}}=5.48$, and $k_{\mu_{al}}=42.41$ (in arbitrary units).

$$E_B(k) = a_{<} \epsilon^{1/2} V_A^{1/2} k_{\eta_{al}}^{13/6} k^{-11/3} \exp\left[-\frac{4}{3} + \frac{3}{2}\left(\frac{k_{\eta_{al}}}{k_{\mu_{un}}}\right)^{4/3}\right] \\ \times \exp\left[-\frac{3}{2}\left(\frac{k}{k_{\mu_{un}}}\right)^{4/3}\right] \quad (k \geq k_{\eta_{al}}). \quad (43)$$

The spectra for E_v and E_B have power laws of $k^{-5/3}$ and $k^{-11/3}$, respectively, with the same exponential falloff governed by viscous dissipation. There is no exponential decay related to resistive dissipation because nonlocal interactions with the flow produce the $11/3$ power law falloff in the range where resistive dissipation is active. The resistive Kolmogorov wavenumber does enter the E_B spectrum through an additional amplitude factor $k_{\eta_{al}}^2$. For $k > k_{\mu_{un}}$ kinetic energy is dissipated on a shorter time scale than nonlinear interactions and all energies decay exponentially. The two spectra are plotted in Fig. 3 for the same parameters as Fig. 2, i.e., $k_{\mu_{un}}=100$, $k_{\eta_{un}}=10$, and $\text{Pm}=4.64 \times 10^{-2}$. Additionally, $\Theta_{k_{\eta_{al}}}=0.30$, yielding $k_{\eta_{al}}=(\Theta_{k_{\eta_{al}}})^{1/2} k_{\eta_{un}}=5.48$ and $k_{\mu_{al}}=(k_{\eta_{un}}/k_{\mu_{un}})^{1/9} (\Theta_{k_{\eta_{al}}})^{1/2} k_{\mu_{un}}=42.41$. Aside from obvious differences in spectra for the $\text{Pm}=1$ and $\text{Pm} \neq 1$ cases, there is not a significant difference in spectra for aligned and unaligned turbulence with the same magnetic Prandtl number.

IV. CONCLUSIONS

We derived turbulent dissipation range spectra for MHD with isotropic viscosity and resistivity using simple closures. We focused on the physics associated with variation of magnetic Prandtl number and alignment of the magnetic and velocity vectors to determine the appropriate exponential spectra that modify power law behavior arising from these effects. Dissipation range spectra have a subrange of exponential falloff beyond the effective Kolmogorov wavenumber. For dimensional reasons the argument of the exponent depends only on physical parameters in the form k/k_{dis} , where k_{dis} is a Kolmogorov wavenumber associated with viscosity or resistivity. The power to which this ratio is raised depends on the rate of spectral energy transfer by the nonlinearity, which in MHD is sensitive to the degree of scale

dependent alignment between fields, and hence the nature of the fluctuation anisotropy. From hydrodynamic theory it is also known that the power of the exponent depends on the way the cubic correlation of the spectral transfer rate is closed to form a representation in terms of quadratic spectrum correlations. This work addressed the effect of different values of the magnetic Prandtl number and the differences in spectra corresponding to aligned turbulence, which has inertial sheetlike fluctuation structure and unaligned turbulence, which has inertial filamentlike structure.

Dissipation range spectra have been formulated for turbulence that is both aligned and unaligned for the inertial scales that feed the dissipation range. For unaligned turbulence with $Pm=1$, the inertial power law $\epsilon^{2/3}k^{-5/3}$ is corrected by an exponential factor $\exp[-(3/2)(k/k_{\eta_{un}})^{4/3}]$, valid for all k , that dominates falloff when the wavenumber exceeds the Kolmogorov wavenumber $k_{\eta_{un}} = \epsilon^{1/4}/\eta^{3/4}$. For aligned turbulence with $Pm=1$ (scale-dependent alignment), the inertial-range power law is $\epsilon^{1/2}V_A^{1/2}k^{-3/2}$. The weaker nonlinearity allows more dissipation in a nonlinear spectral transfer time, yielding a stronger exponential correction $\exp[-(4/3) \times (k/k_{\eta_{al}})^{3/2}]$ in the inertial range $k < k_{\eta_{al}}$, where $k_{\eta_{al}} = \epsilon^{1/3}/V_A^{1/3}\eta^{1/3}$. In the dissipation range $k > k_{\eta_{al}}$, simulations indicate that the alignment angle ceases to decrease with k but is frozen at its value for $k=k_{\eta_{al}}$. Hence for this range, the turbulence, while aligned, is scale independent and spectral decay has the same wavenumber variation as unaligned turbulence, with factors of $k^{-5/3}$ and $\exp[-(3/2)(k/k_{\eta_{un}})^{4/3}]$. Equal dissipation of magnetic and kinetic energies carries inertial structures into the dissipation range unaltered in shape.

For $Pm < 1$ we have derived spectra that describe the transition from the inertial to the dissipation range for turbulence with and without scale-dependent alignment. In both cases, the small-scale limit has exponential falloff governed by viscous dissipation with a form characteristic of unaligned structure, $\exp[-(3/2)(k/k_{\mu_{un}})^{4/3}]$. This reflects turbulence that is essentially Kolmogorov with a parasitic magnetic field. Hence, there is a power law factor of $k^{-5/3}$ for the kinetic energy and $k^{-11/3}$ for magnetic energy. Alignment only affects the spectrum in the inertial range, resulting in different large-scale asymptotes for aligned and unaligned turbulence. These include the characteristic power law factors of $k^{-3/2}$ and $k^{-5/3}$ for aligned and unaligned turbulence. For magnetic energy the corresponding exponential correction factors are $\exp[-(4/3)(k/k_{\eta_{al}})^{3/2}]$ and $\exp[-(3/2) \times (k/k_{\eta_{un}})^{4/3}]$, respectively, reflecting differing amounts of dissipation in a transfer time scale. The exponential factors of large-scale behavior for the kinetic energy are the same but with the viscous wavenumbers $k_{\mu_{al}}$ and $k_{\mu_{un}}$ in place of the resistive wavenumbers. The details of these spectral forms are less significant than the general insight that alignment and differences in dissipation rates lead to differences in dissipation range spectra, including Kolmogorov wavenumbers.

The Madison Symmetric Torus (MST) reversed field pinch³² has magnetic turbulence that is relevant to the $Pm < 1$ limit. (The magnetic Prandtl number in MST is on the

order of 0.01 for the viscosity associated with diffusion of perpendicular flow in the direction perpendicular to the mean field, as calculated from the appropriate components of the Braginskii pressure tensor for MST parameters.) An exponential spectrum has been observed using magnetic probes.³³ However, the entire spectrum covers a range of scales that are considerably larger than the resistive Kolmogorov scale (using either $k_{\eta_{al}}$ or $k_{\eta_{un}}$ as an estimate). Because cyclotron resonances do fall within the spectrum, the exponential behavior may result from kinetic dissipation.^{33,34} These issues will be considered elsewhere. Dissipation range spectra for $Pm > 1$ is also left to future work.

ACKNOWLEDGMENTS

Useful discussions with Derek Baver, Stanislav Boldyrev, John Sarff, Abulgader Almagri, Yang Ren, and Gennady Fiksel are acknowledged. This work was supported by the National Science Foundation and the U.S. Department of Energy.

- ¹R. J. Leamon, C. W. Smith, N. F. Ness, W. H. Matthaeus, and H. K. Wong, *J. Geophys. Res.* **103**, 4775, DOI: 10.1029/97JA03394 (1998).
- ²C. W. Smith, K. Hamilton, B. J. Vasquez, and R. J. Leamon, *Astrophys. J. Lett.* **645**, L85 (2006).
- ³C. C. Chaston, C. Salem, J. W. Bonnell, C. W. Carlson, R. E. Ergun, R. J. Strangeway, and J. P. McFadden, *Phys. Rev. Lett.* **100**, 175003 (2008).
- ⁴L. Marrelli, L. Frassineti, P. Martin, D. Craig, and J. S. Sarff, *Phys. Plasmas* **12**, 030701 (2005).
- ⁵P. W. Terry, C. McKay, and E. Fernandez, *Phys. Plasmas* **8**, 2707 (2001).
- ⁶S. D. Bale, P. J. Kekhogg, F. S. Mozer, T. S. Horbury, and H. Reme, *Phys. Rev. Lett.* **94**, 215002 (2005).
- ⁷G. G. Howes, S. C. Cowley, W. Dorland, G. W. Hammett, E. Quataert, and A. A. Schekochihin, *Astrophys. J.* **651**, 590 (2006).
- ⁸U. Frisch, *Turbulence* (Cambridge University Press, Cambridge, 1995).
- ⁹G. G. Howes, S. C. Cowley, W. Dorland, G. W. Hammett, E. Quataert, and A. A. Schekochihin, *J. Geophys. Res.* **113**, A05103, DOI: 10.1029/2007JA012665 (2008).
- ¹⁰D. Biskamp, *Nonlinear Magnetohydrodynamics* (Cambridge University Press, Cambridge, 1993).
- ¹¹S. Boldyrev, *Astrophys. J. Lett.* **626**, L37 (2005).
- ¹²P. Goldreich and S. Sridhar, *Astrophys. J.* **438**, 763 (1995).
- ¹³G. S. Golitsyn, Sov. Phys. Dokl. **5**, 536 (1960).
- ¹⁴K. Moffatt, *J. Fluid Mech.* **11**, 625 (1961).
- ¹⁵D. Biskamp and W.-C. Muller, *Phys. Plasmas* **7**, 4889 (2000).
- ¹⁶J. J. Podesta, B. D. G. Chandran, A. Bhattacharjee, D. A. Roberts, and M. L. Goldstein, *J. Geophys. Res.* **114**, A01107, DOI: 10.1029/2008JA013504 (2009).
- ¹⁷J. Mason, F. Cattaneo, and S. Boldyrev, *Phys. Rev. E* **77**, 036403 (2008).
- ¹⁸A. A. Townsend, *Proc. R. Soc. London, Ser. A* **208**, 534 (1951).
- ¹⁹S. Corrsin, *Phys. Fluids* **7**, 1156 (1964).
- ²⁰Y. H. Pao, *Phys. Fluids* **8**, 1063 (1965).
- ²¹H. Tennekes and J. L. Lumley, *A First Course in Turbulence* (MIT, Cambridge, 1972).
- ²²R. H. Kraichnan, *J. Fluid Mech.* **5**, 497 (1959).
- ²³C. Foias, O. Manley, and L. Sirovich, *Phys. Fluids A* **2**, 464 (1990).
- ²⁴A. S. Monin and A. M. Yaglom, *Statistical Fluid Mechanics* (MIT, Cambridge, 1975), Vol. II.
- ²⁵L. M. Smith and W. C. Reynolds, *Phys. Fluids A* **3**, 992 (1991).
- ²⁶L. M. Smith, private communication (2008).
- ²⁷J. Mason, F. Cattaneo, and S. Boldyrev, *Phys. Rev. Lett.* **97**, 255002 (2006).
- ²⁸S. I. Braginskii, *Rev. Plasma Phys.* **1**, 205 (1965).
- ²⁹P. S. Iroshnikov, Sov. Astron. **7**, 566 (1964).

³⁰R. H. Kraichnan, *Phys. Fluids* **8**, 1385 (1965).

³¹G. K. Batchelor, *The Theory of Homogeneous Turbulence* (Cambridge University Press, Cambridge, 1953).

³²S. C. Prager, A. F. Almagri, S. Assadi, J. A. Beckstead, R. N. Dexter, D. J. Den Hartog, G. Chartas, S. A. Hokin, T. W. Lovell, T. D. Rempel, J. S.

Sarff, W. Shen, C. W. Spragins, and J. C. Sprott, *Phys. Fluids B* **2**, 1367 (1990).

³³P. W. Terry, V. Tangri, J. S. Sarff, G. Fiksel, A. F. Almagri, Y. Ren, and S. C. Prager, *Fusion Energy* **2008**, TH-P8-43 (2008).

³⁴V. Tangri, P. W. Terry, and G. Fiksel, *Phys. Plasmas* **15**, 112501 (2008).